Two-body correlations from $(e, e'd)$ reactions: ^{4}He$(e, e'd)^2$H as a test case

Winfried Leidemann
European Center for Theoretical Nuclear Physics and Related Areas, Villa Tambosi, I-38050 Villazzano (Trento), Italy

Giuseppina Orlandini and Marco Traini
Dipartimento di Fisica, Università di Trento, I-38050 Povo (Trento), Italy

Edward L. Tomusiak
Linear Accelerator Laboratory and Department of Physics, University of Saskatchewan, Saskatoon, Canada S7N 0W0
(Received 30 November 1993)

The utility of $(e, e'd)$ reactions in providing information about dynamical correlations in nuclei is discussed. The breakup of ^{4}He into two deuterons is taken as a model case. We show how two-nucleon dynamics of both short range and tensor nature affects the $(e, e'd)$ cross section in different kinematical regions. The role of final state interactions is also discussed. Within our model, kinematical conditions can be chosen to emphasize the sensitivity to a particular aspect of the ground state dynamics thereby suggesting promising avenues for experiment.

PACS number(s): 21.45.+v, 25.30.Fj, 27.10.+h

I. INTRODUCTION

Electron induced two-body knock-out reactions appear to offer the most direct route to studying nucleon-nucleon correlations in nuclei [1]. The two-nucleon emission process provides richer and more direct information on NN dynamics than does the one nucleon knock-out process. In fact it is evident that one-body knock-out reactions reflect the two-nucleon dynamics only in an integrated way. Nevertheless $(e, e'NN)$ experiments are difficult because they involve triple coincidences. However, an interesting exception occurs in the $(e, e'd)$ reaction which was previously suggested as a tool for investigating short range correlations [2–8].

The viewpoint most often taken regarding dynamical correlations is that they are given by the difference between the true two-body density and the one of an independent particle model (IPM). In this picture the IPM is considered the approximation wherein the sole effect of NN interactions has been to establish a mean field. What is missing then are two-body and higher order correlations which do not allow the wave function to be expressible as a single Slater determinant. For example, dynamical NN correlations would appear as an infinite sum of Slater determinants describing the scattering of a pair of particles in an occupied orbital to orbitals far above the Fermi surface.

Clearly what is required in order to experimentally study correlations is direct access to the two-body density. As is well known this is not easy and, even if one did have such access, there would still remain uncertainties because the free two-body density is not an observable. That is, the extraction of the dynamical part of the two-body density would not necessarily be straightforward. In principle the integrated strength of the longitudinal form factor can give direct knowledge of the two-body density. There are obvious experimental difficulties with this approach although it has been carried out for ^{3}He [9]. It has been shown [4] that $(e, e'NN)$ or $(e, e'd)$ cross sections could provide direct information on the two-hole spectral function only by invoking rather severe assumptions. In fact, as opposed to the case of one-body knock-out reactions, here the neglect of final state interactions (FSI's) and proper antisymmetrization still does not permit a factorization of the cross section. Rather, to obtain factorization one requires the additional approximation of zero-range NN interactions [10]. This is an unacceptable condition for a formalism designed to help investigate just that question, namely, the nature of NN correlations in nuclei.

Cognizant of these difficulties we adopt a different approach in our study of correlations from the two-body knock-out cross sections. We calculate and compare two cross sections: one obtained within the assumption that the nucleons move nearly independently and one in which some model correlations are superimposed on top of this independent motion. In addition all other conditions such as FSI's can be fixed. By nearly independent motion we mean that the model properly includes the effects of antisymmetrization and center of mass motion. Thus there are already minimal two-body correlations present in our nearly independent motion model, namely, those due to Pauli and center of mass motion. In this way we avoid the ambiguities related to the (non)factorization of the cross section and hence we can check various kinematical regimes for sensitivity to the additional short range and tensor correlations.

The aim of this work is to study in a model case the sensitivity of the $(e, e'd)$ cross section to dynamical correlations. Various kinematical regions are explored in order to find those where particular aspects of the ground state dynamics dominate the cross section. At the same time the influence of FSI's is analyzed to understand whether or not they can mask ground state correlation effects. All

this is done in the model case of ^{4}He$(e,e'd)d$. The choice of this reaction stems from the following two considerations. First, as already mentioned, the concept of correlations applies to systems for which the IPM represents — with c.m. corrections — a reasonable approximation. In our view ^{4}He is the lightest and therefore simplest system where this is true. Second, in order to simplify the study of FSI's, a reaction in which the $(A-2)$ system remains in its ground state is preferred.

Although we do not expect the model presented here to be realistic enough to permit a serious comparison of our results to data, it may nevertheless be a useful guide to future investigations of $(e,e'd)$ knock-out from heavier systems. Our model is simple but we have constrained it to be as realistic as possible. This is accomplished by choosing parameters so that quantities like elastic form factors and asymptotic D/S ratios compare favorably with the corresponding quantities from experimental data or more realistic few-body calculations. However our treatment of FSI's is at best rudimentary and important effects such as inelasticities due to channel coupling are neglected.

II. FORMALISM

In general the $(e,e'd)$ cross section can be written as

$$\frac{d^5\sigma}{de_{k'}d\Omega_{k'}d\Omega_d} = \sigma_{\rm Mott}\left(\frac{M_d p}{2}\right)\frac{1}{1-(q/2p)\cos(\theta_{pq})}(V_L F_L + V_T F_T + V_{LT}F_{LT} + V_{TT}F_{TT}), \tag{1}$$

where $e_{k'}$ and $\Omega_{k'}$ are the scattered electron energy and solid angle, Ω_d and p are the laboratory system solid angle and momentum of the detected deuteron, q is the magnitude of the three-momentum transfer of the scattered electron, and θ_{pq} is the angle between $\mathbf{p}$ and $\mathbf{q}$. The kinematical factors V are defined as

$$V_L = \frac{q_\mu^4}{q^4}\,,\quad V_T = \frac{q_\mu^2}{2q^2} + tg^2\left(\frac{\theta_e}{2}\right)\,, \tag{2}$$

$$V_{LT} = \frac{1}{\sqrt{2}}\frac{q_\mu^2}{q^2}\sqrt{\frac{q_\mu^2}{q^2} + tg^2\left(\frac{\theta_e}{2}\right)}\,,\quad V_{TT} = \frac{-q_\mu^2}{2q^2}\,, \tag{3}$$

where q_μ and θ_e are the electron four-momentum transfer and scattering angle, respectively, and where the structure functions F are given by

$$F_L = |\langle f|\rho|i\rangle|^2\,,\quad F_T = |\langle f|J_+|i\rangle|^2 \;+\; |\langle f|J_-|i\rangle|^2\,, \tag{4}$$

$$F_{LT} = -2{\rm Re}\langle f|\rho^\dagger|i\rangle\langle i|J_+ - J_-|f\rangle\,,\quad F_{TT} = 2{\rm Re}\langle f|J_+^\dagger|i\rangle\langle i|J_-|f\rangle\,. \tag{5}$$

Here ρ and $\mathbf{J}$ are the nuclear charge and current operators, respectively, and

$$J_\pm \;=\; \mp\frac{1}{\sqrt{2}}(J_x \;\pm\; iJ_y)\,. \tag{6}$$

Antisymmetry of the wave functions allows one to write the matrix elements $\langle f|J_\mu|i\rangle$ as sums of direct and exchange terms:

$$\langle f|J_\mu|i\rangle = \sqrt{2A(A-1)}\left[D + \frac{A-2}{2}E\right]. \tag{7}$$

With a choice of coordinates where the nucleus c.m. coordinate is $\mathbf{R}$, the displacement between particles A and $(A-1)$ is $\mathbf{x}$, the displacement between the center of mass of those two particles and that of the $(A-2)$ system is $\mathbf{y}$, and the Jacobi coordinates $\boldsymbol{\xi}_1, \boldsymbol{\xi}_2, \ldots, \boldsymbol{\xi}_{A-3}$ are relative coordinates of particles in the $A-2$ system, D and E assume the following forms:

$$D = \sum_\beta \langle \Phi_\beta^f(\mathbf{x},\mathbf{y})\Psi_\beta(\boldsymbol{\xi}_1,\boldsymbol{\xi}_2,\ldots,\boldsymbol{\xi}_{A-3})|e^{-i\frac{1}{2}\mathbf{q}\cdot\mathbf{x}}e^{-i\frac{A-2}{A}\mathbf{q}\cdot\mathbf{y}}J_\mu(A)|i\rangle\,, \tag{8}$$

$$E = \sum_\beta \langle \Phi_\beta^f(\mathbf{x},\mathbf{y})\Psi_\beta(\boldsymbol{\xi}_1,\boldsymbol{\xi}_2,\ldots,\boldsymbol{\xi}_{A-3})|e^{i\frac{2}{A}\mathbf{q}\cdot\mathbf{y}}e^{i\frac{A-3}{A-2}\mathbf{q}\cdot\boldsymbol{\xi}_{A-3}}J_\mu(A-2)|i\rangle\,, \tag{9}$$

where $\Psi_\beta(\boldsymbol{\xi}_1,\boldsymbol{\xi}_2,\ldots,\boldsymbol{\xi}_{A-3})$ are the antisymmetric eigenfunctions of the $(A-2)$-particle Hamiltonian, and $\Phi_\beta^f(\mathbf{x},\mathbf{y})$

the projections of the final state on $\Psi_\beta(\boldsymbol{\xi}_1,\boldsymbol{\xi}_2,\ldots,\boldsymbol{\xi}_{A-3})$, i.e.,

$$\Phi^f_\beta(\mathbf{x},\mathbf{y}) = \int d\boldsymbol{\xi}_1\cdots d\boldsymbol{\xi}_{A-3}\Psi^\star_\beta(\boldsymbol{\xi}_1,\boldsymbol{\xi}_2,\ldots,\boldsymbol{\xi}_{A-3})\Psi_f(\mathbf{x},\mathbf{y},\boldsymbol{\xi}_1,\boldsymbol{\xi}_2,\ldots,\boldsymbol{\xi}_{A-3})\ . \tag{10}$$

The one-body current operators $J_\mu(n)$ are $\frac{1}{2}[1+\tau_3(n)]$ for the charge ρ, $\frac{1}{2}[1+\tau_3(n)](-i/m)\boldsymbol{\nabla}(n)$ for the convection current, and $i\mathbf{q}\times[\mu_s+\mu_v\tau_3(n)]\boldsymbol{\sigma}(n)$ for the spin current. Specializing to the case of the ^{4}He$(e,e'd)d$ reaction, the residual $A-2$ system is simply a deuteron so that $\Psi_\beta(\boldsymbol{\xi}_1,\boldsymbol{\xi}_2,\ldots,\boldsymbol{\xi}_{A-3})$ becomes $d_M(\mathbf{x})$, a deuteron wave function with spin projection M. Then

$$\Phi^f_\beta(\mathbf{x},\mathbf{y}) \equiv \Phi^f_0(\mathbf{x},\mathbf{y}) = d_M(\mathbf{x})\chi^{(-)}_\kappa(\mathbf{y})\,, \tag{11}$$

where $\chi^{(-)}_\kappa(\mathbf{y})$ is the asymptotic ingoing wave of the two deuterons with relative momentum κ. Thus, in this case,

$$D = \langle d_M(\mathbf{x})d_{M'}(\boldsymbol{\xi})\chi^{(-)}_k(\mathbf{y})|e^{i\frac{\mathbf{q}}{2}\cdot\mathbf{x}}e^{i\frac{\mathbf{q}}{2}\cdot\mathbf{y}}J_\mu(A)|\alpha\rangle\,, \tag{12}$$

where $|\alpha\rangle$ represents the ^{4}He ground state. The exchange term E is obtained by the replacements

$$E = D\,[\mathbf{y}\to-\mathbf{y};\mathbf{x}\to-\boldsymbol{\xi}]\ . \tag{13}$$

In the following we describe our model in detail and then give explicit expressions for D and E.

III. DESCRIPTION OF THE MODEL

A. Ground state model

We want to allow for both NN correlations as well as a D-state component in the ^{4}He ground state. The correlated S-wave part is taken as

$$\Psi_S(\alpha,\gamma) \;=\; N_0\prod_{i<j} f(r_{ij},\gamma)\;\Phi_0(\alpha)\,, \tag{14}$$

where N_0 is a normalization constant, the Jastrow function is of Gaussian form

$$f(r_{ij},\gamma) \;=\; 1 \;-\; e^{-\gamma\alpha^2 r^2_{ij}}\,, \tag{15}$$

and $\Phi_0(\alpha)$ is the relative wave function corresponding to four nucleons in a harmonic oscillator $0S$ orbital. Thus,

$$\Phi_0(\alpha) \;=\Psi\left(\frac{\alpha\mathbf{x}}{\sqrt{2}}\right)\Psi\left(\frac{\alpha\boldsymbol{\xi}}{\sqrt{2}}\right)\Psi(\alpha\mathbf{y})\,|[1]^4\ S=0\ T=0\rangle\,, \tag{16}$$

where

$$\Psi(\alpha\mathbf{z}) = R_0(z)Y_{00}(\hat{z}) = \sqrt{\frac{4\alpha^3}{\sqrt{\pi}}}e^{-\frac{1}{2}\alpha^2z^2}Y_{00}(\hat{z})\,. \tag{17}$$

The relative coordinates are defined through

$$\mathbf{x} = \mathbf{r}_3 - \mathbf{r}_4\ , \tag{18a}$$

$$\mathbf{y} = \frac{1}{2}(\mathbf{r}_1+\mathbf{r}_2-\mathbf{r}_3-\mathbf{r}_4)\ , \tag{18b}$$

$$\boldsymbol{\xi} = \mathbf{r}_2-\mathbf{r}_1\ , \tag{18c}$$

or, in terms of particle coordinates $\mathbf{r}_i$ and the usual c.m. coordinate $\mathbf{R}$,

$$\mathbf{r}_1 \;=\; \mathbf{R}+\tfrac{1}{2}\mathbf{y}-\tfrac{1}{2}\boldsymbol{\xi}\ , \tag{19a}$$

$$\mathbf{r}_2 \;=\; \mathbf{R}+\tfrac{1}{2}\mathbf{y}+\tfrac{1}{2}\boldsymbol{\xi}\ , \tag{19b}$$

$$\mathbf{r}_3 \;=\; \mathbf{R}-\tfrac{1}{2}\mathbf{y}+\tfrac{1}{2}\mathbf{x}\ , \tag{19c}$$

$$\mathbf{r}_4 \;=\; \mathbf{R}-\tfrac{1}{2}\mathbf{y}-\tfrac{1}{2}\mathbf{x}\ . \tag{19d}$$

Next a D-wave component is introduced into the alpha particle ground state. To do this we follow the method Gerjuoy and Schwinger [11]. These authors did not use isospin formalism, and so we have to modify their method accordingly. Specifically if one defines

$$\boldsymbol{\sigma}_{ij} = \boldsymbol{\sigma}(i)-\boldsymbol{\sigma}(j)\,, \tag{20}$$

then the operator

$$\hat{M} = (\boldsymbol{\sigma}_{12}\cdot\boldsymbol{\xi})(\boldsymbol{\sigma}_{34}\cdot\mathbf{x})+(\boldsymbol{\sigma}_{12}\cdot\mathbf{x})(\boldsymbol{\sigma}_{34}\cdot\boldsymbol{\xi})-\frac{2}{3}(\mathbf{x}\cdot\boldsymbol{\xi})(\boldsymbol{\sigma}_{12}\cdot\boldsymbol{\sigma}_{34})\,, \tag{21}$$

acting on a state with $L=S=J=0$, yields a state with $L=S=2$ and $J=0$. An antisymmetric wave function is obtained then by the linear combination

$$\begin{aligned}|\Psi_D(\alpha',\gamma')\rangle &= N_D\ [1+(14)+(13)]\ \hat{M}\ |\Psi_S(\alpha',\gamma')\rangle\\ &= N_D\hat{M}_{\rm eff}\ |\Psi_S(\alpha',\gamma')\rangle\,,\end{aligned} \tag{22}$$

where (ij) is a permutation operator and N_D is a normalization constant determined from

$$\begin{aligned}1 = \langle\Psi_D(\alpha',\gamma')|\Psi_D(\alpha',\gamma')\rangle &= N^2_D\langle\Psi_S(\alpha',\gamma')|\hat{M}^\dagger_{\rm eff}\hat{M}_{\rm eff}|\Psi_S(\alpha',\gamma')\\ &= 4\ N^2_D\langle\Psi_S(\alpha',\gamma')|\mathcal{N}(\mathbf{x},\boldsymbol{\xi},\mathbf{y})|\Psi_S(\alpha',\gamma')\rangle\,,\end{aligned} \tag{23}$$

where

$$\mathcal{N}(\mathbf{x},\boldsymbol{\xi},\mathbf{y}) = \xi^4 + x^4 + 16y^4 + 6(\boldsymbol{\xi}\cdot\mathbf{x})^2 - 12(\boldsymbol{\xi}\cdot\mathbf{y})^2 - 12(\mathbf{x}\cdot\mathbf{y})^2 + 8\xi^2x^2 + 4\xi^2y^2 + 4x^2y^2 \ . \tag{24}$$

For the noncorrelated case, i.e., $\Psi_S(\alpha',\gamma') = \Phi_0(\alpha')$, one obtains

$$N_D = \frac{\alpha'^2}{2\sqrt{192}} \ . \tag{25}$$

In Eq. (22) we have allowed for possibly different oscillator and Jastrow parameters than what is used in the S-wave part. Finally the mixing between S and D states is included by a mixing angle ϵ. Thus our model for the alpha particle is now

$$\Psi(^4\mathrm{He}) = \cos(\epsilon)\Psi_S(\alpha,\gamma) + \sin(\epsilon)\Psi_D(\alpha',\gamma') \ . \tag{26}$$

The ground state wave function described above contains several parameters which need to be constrained in some reasonable fashion. First we set the D-wave parameters α' and γ' equal to the S-wave parameters α and γ. There is no reason other than simplicity for making this assumption. Neither the S-wave nor D-wave spatial distributions bear any relation to the one-pion-exchange component of the N-N potential. Nevertheless, as we will see at the end of this paragraph, our model leads to reasonable results for the static ^{4}He properties of Figs. 1 and 2. Still there remain four parameters, e.g., α, γ, ϵ, and the sign of ϵ. Our procedure is as follows: For a fixed value of ϵ or equivalently, percent D wave, we adjust α and γ to obtain the ^{4}He charge radius of $\langle r^2\rangle_{\mathrm{ch}}$= 2.80 fm^2 and in addition we fix the position of the first diffraction minimum at q^2 = 10, 13, and 16 fm^{-2}. That is, for a given D-wave percentage, we have three sets of (α,γ) which each give the correct nuclear size but correspond to Jastrow correlations of varying strength, the set giving the form factor minimum at q^2=10 fm^{-2} being the strongest. In detail the model charge radius is computed from

$$\begin{aligned}\langle \mathbf{R}^2_{\mathrm{chg}}\rangle &= \langle\Psi(^4\mathrm{He})|\frac{1}{Z}\sum_i[\mathbf{r}(i)-\mathbf{R}]^2\ \frac{1}{2}[1+\tau_3(i)]|\Psi(^4\mathrm{He})\rangle \\ &= \langle\Psi(^4\mathrm{He})|\frac{1}{4}(x^2+y^2+2\mathbf{x}\cdot\mathbf{y})|\Psi(^4\mathrm{He})\rangle \\ &= \cos^2(\epsilon)\langle\Psi_S(\alpha,\gamma)|\frac{1}{4}(x^2+y^2+2\mathbf{x}\cdot\mathbf{y})|\Psi_S(\alpha,\gamma)\rangle \\ &\quad +4N_D^2\sin^2(\epsilon)\langle\Psi_S(\alpha,\gamma)|\frac{1}{4}(x^2+y^2+2\mathbf{x}\cdot\mathbf{y})\mathcal{N}(\mathbf{x},\boldsymbol{\xi},\mathbf{y})|\Psi_S(\alpha,\gamma)\rangle \ .\end{aligned} \tag{27}$$

Since we take the proton radius as $\langle r_p^2\rangle$=0.64 fm^2 the value of $\langle \mathbf{R}^2_{\mathrm{chg}}\rangle$ is set to 2.16 fm^2. Similarly the model elastic charge form factor is obtained by the replacement

$$\frac{1}{4}(x^2+y^2+2\mathbf{x}\cdot\mathbf{y}) \ \rightarrow \ e^{i\frac{1}{2}\mathbf{q}\cdot(\mathbf{x}+\mathbf{y})} \tag{28}$$

in Eq. (27). Since the wave functions and correlation functions are Gaussians, the integrals required can be performed analytically. A symbolic logic program, MATHEMATICA, was used to keep track of the algebra. Thus there is no truncation of the correlation function in the calculations described here. Figure 1 illustrates the elastic charge form factors corresponding to P_D=10%. We note that even more realistic calculations [12] cannot describe the high-q form factor with only a one-body charge operator.

The above criteria do not determine the sign of the mixing angle. However, the experimental determination of the parameter D_2, which is related to the asymptotic ratio of the radial D- and S-wave functions in the $d+d$ amplitude, suggests a definite sign, which according to our definitions corresponds to a positive mixing angle ϵ. The D_2 value is given by

$$D_2 = -\sqrt{\frac{5}{3}}\lim_{k\to 0}\frac{1}{k^2}\frac{A^{22}_{dd}(-1,-1,k)}{A^{00}_{dd}(0,0,k)} \ , \tag{29}$$

with

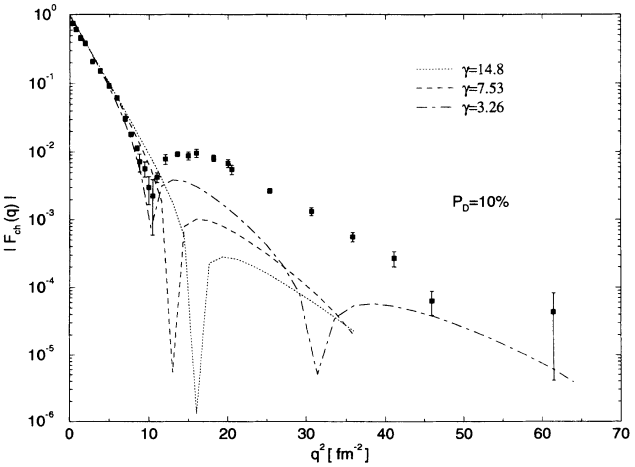

FIG. 1. Charge form factor of ^{4}He for the models with P_D = 10%: model 4 (dotted curve), model 3 (dashed curve), model 2 (dash-dotted curve). Experimental data from [19,20].

$$A_{dd}^{lm}(M,M',k) = 4\pi\sqrt{3}\,\langle d_M(\mathbf{x}) d_{M'}(\boldsymbol{\xi})\, Y_{lm}(\Omega_y) j_l(ky) | \Psi(^4\mathrm{He})\rangle\,. \tag{30}$$

The results for D_2 with positive ϵ and the parameter values for the various models are listed in Table I. One notes that all D_2 values are compatible with the experimental result of -0.3 ± 0.1 fm^2 [13]. To further demonstrate that our D-state model is not much at variance with more realistic models Fig. 2 compares our $A_{dd}^{00}(0,0,k)$ and $A_{dd}^{22}(-1,-1,k)$ amplitudes to those obtained using more realistic ^{4}He wave functions [14]. Thus we are confident that the parameter sets shown in Table I will enable us to study the $^4\mathrm{He}(e,e'd)d$ reaction systematically with respect to ground state properties such as short range correlations and D-wave content.

B. Final state model

The final state we consider is an incoming wave corresponding to two deuterons with asymptotic relative momentum $\boldsymbol{\kappa}$, i.e.,

$$\langle \mathbf{x},\mathbf{y},\boldsymbol{\xi}\,|\boldsymbol{\kappa}, MM'\rangle^{(-)} = d_M(\mathbf{x}) d_{M'}(\boldsymbol{\xi}) \chi_{\boldsymbol{\kappa}}^{(-)}(\mathbf{y})\,, \tag{31}$$

where in the limit of no final state interactions between the outgoing deuterons one has simply

$$\chi_{\boldsymbol{\kappa}}^{(-)}(\mathbf{y}) \rightarrow \tfrac{1}{\sqrt{8\pi^3}} e^{i\boldsymbol{\kappa}\cdot\mathbf{y}}\,. \tag{32}$$

Our estimates of the effects of final state interactions will adopt the method of [15,16] in which $\chi_{\boldsymbol{\kappa}}^{(-)}(\mathbf{y})$ is constructed from a d-d cluster model employing a Woods-Saxon potential. In essence this just means that we make the replacement

$$j_L(\kappa y) \rightarrow R_L(\kappa, y)\, e^{i\delta_L}\,, \tag{33}$$

where $R_L(\kappa,y)$ is the Lth partial wave in the Woods-Saxon potential. This model for the FSI is primitive. A proper many-body calculation would include the coupling of the $d+d$ state to other channels such as the (3+1) and (2+1+1) channels. Such calculations, using modern potential models, are only now becoming feasible for the three-nucleon system and are not yet practical for the four-nucleon problem. In the meantime we hope that our treatment of the (2+2)-body breakup channel alone may provide a useful guide to the importance of the FSI and ground state correlations.

For the deuteron wave functions d_M we take

TABLE I. Model parameters, position of elastic form factor minimum ($q^2_{\min}$) , and asymptotic D/S ratio D_2.

	Model 1	Model 2	Model 3	Model 4	Model 5
γ	7.596	3.264	7.533	14.784	7.860
α [fm^{-1}]	0.7382	0.7815	0.7531	0.7437	0.7667
P_D [%]	0	10	10	10	20
N_0	1.0776	1.2628	1.0786	1.0294	1.0739
N_D	-	0.0203	0.0203	0.0203	0.0211
$q^2_{\min}$ [fm^{-2}]	13.0	10.0	13.0	16.0	13.0
D_2 [fm^2]	0	-0.21	-0.23	-0.24	-0.33

$$d_M(\mathbf{x}) = \left[U(x) + \frac{1}{\sqrt{8}} W(x)\, S_{12}\right] \chi_M^1\, \eta_0^0\,, \tag{34}$$

where $U(x) = u(x)/x$ and $W(x) = w(x)/x$ are obtained from the Paris potential [17] and S_{12} denotes the tensor operator.

C. Transition matrix elements

The direct and exchange parts of the matrix element of the charge operator

$$^{(-)}\langle \boldsymbol{\kappa},\, MM' \,|\, \rho \,|\, \Psi(^4\mathrm{He})\rangle = \sqrt{24}\,[D_{MM'}(\rho) + E_{MM'}(\rho)] \tag{35}$$

are given by

$$D_{MM'}(\rho) = \frac{1}{2}\, ^{(-)}\langle \boldsymbol{\kappa},\, MM' \,|\, e^{-\frac{i}{2}\mathbf{q}\cdot(\mathbf{x}+\mathbf{y})} \,|\, \Psi(^4\mathrm{He})\rangle\,, \tag{36}$$

$$E_{MM'}(\rho) = \frac{1}{2}\, ^{(-)}\langle \boldsymbol{\kappa},\, MM' \,|\, e^{+\frac{i}{2}\mathbf{q}\cdot(\boldsymbol{\xi}+\mathbf{y})} \,|\, \Psi(^4\mathrm{He})\rangle\,, \tag{37}$$

where we have used the fact that only the isoscalar part can contribute to this process. A relationship between direct and exchange parts can be obtained after invoking

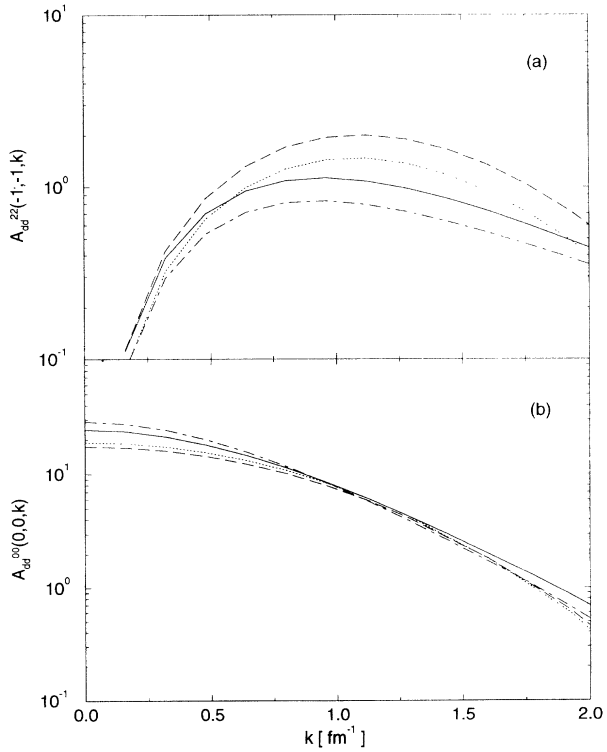

FIG. 2. The amplitudes $A_{dd}^{22}(-1,-1,k)$ (a) and $A_{dd}^{00}(0,0,k)$ (b) for models 3 (dotted curve) and 5 (dashed curve). The results for potential models of Argonne (dash-dotted curve) and Urbana type (solid curve) from [14].

the various permutation and parity properties of the wave functions. One obtains

$$E_{MM'}(\rho) = \frac{1}{2}\,{}^{(-)}\langle \boldsymbol{\kappa},\, MM' \,|\, e^{-\frac{i}{2}\mathbf{q}\cdot(\mathbf{x}-\mathbf{y})} \,|\, \Psi(^4\mathrm{He})\rangle\,, \quad (38)$$

which is almost the same as $D_{M'M}$ except for the sign of $\mathbf{y}$ in the exponential.

To calculate the charge matrix elements one has to perform the following nine-dimensional integration:

$$D_{MM'}(\rho) + E_{MM'}(\rho) = \int\int\int d^3x\, d^3\xi\, d^3y\, \chi_\kappa^{(-)}(\mathbf{y}) \left(e^{-\frac{i}{2}\mathbf{q}\cdot(\mathbf{x}+\mathbf{y})} + e^{+\frac{i}{2}\mathbf{q}\cdot(\boldsymbol{\xi}+\mathbf{y})}\right) \times \left[\cos(\epsilon)\mathcal{M}^S_{MM'} + N_D \sin(\epsilon)\mathcal{M}^D_{MM'}\right] \Psi_S(\alpha,\gamma)\,, \quad (39)$$

where

$$\mathcal{M}^{S/D}_{MM'} = \frac{1}{2}\langle MM' \,|\, \hat{M}^{S/D}_{\mathrm{eff}} \,|\, [1]^4\, S=0\, T=0\rangle \quad (40)$$

denotes the spin and isospin dependent piece. Note that $\hat{M}^D_{\mathrm{eff}}$ is defined in Eq. (22), while $\hat{M}^S_{\mathrm{eff}} = 1$. The matrix elements fulfill the following symmetry relations:

$$\mathcal{M}^*_{MM'} = (-)^{M+M'}\mathcal{M}_{-M-M'}\,, \quad (41)$$

$$\mathcal{M}_{M'M} = \mathcal{M}_{MM'}(\mathbf{x} \leftrightarrow \boldsymbol{\xi})\,. \quad (42)$$

Because of these relations, it is sufficient to give explicit results for the matrix elements with $(MM') = (1-1)$, (0,0), (0,1), and (1,1).

For the S-wave part only three combinations of M and M' lead to nonvanishing results $[(1-1),(-11),(00)]$. In detail one finds

$$\mathcal{M}^S_{1-1} = \frac{1}{8\sqrt{3}}\left[\frac{U(x)U(\xi)}{\sqrt{2\pi}} + \frac{V_0(\mathbf{x},\boldsymbol{\xi})}{\sqrt{5\pi}}\right] + \frac{W(x)W(\xi)}{20\sqrt{6}}\sum_{m=0}^{2}(-)^m\left[3m + \delta_{m0}(1-3m)\right] Y_{2m}(\hat{x})Y_{2-m}(\hat{\xi}) \quad (43)$$

and

$$\mathcal{M}^S_{00} = \mathrm{Re}\left(\frac{1}{4\sqrt{3}}\left[-\frac{U(x)U(\xi)}{2\sqrt{2\pi}} + \frac{V_0(\mathbf{x},\boldsymbol{\xi})}{\sqrt{5\pi}}\right] + \frac{\sqrt{6}}{10}W(x)W(\xi)\sum_{m=0}^{1}\frac{(-)^{m+1}}{3-m}Y_{2m}(\hat{x})Y_{2-m}(\hat{\xi})\right)\,, \quad (44)$$

where we have introduced

$$V_m(\mathbf{x},\boldsymbol{\xi}) = U(x)W(\xi)Y_{2m}(\hat{\xi}) + W(x)U(\xi)Y_{2m}(\hat{x})\,. \quad (45)$$

The nine matrix elements of the D-wave part generally have the form

$$\mathcal{M}^D_{MM'} = \sum_{m=-2}^{2}\left[x^2Y_{2m}(\hat{x}) + \xi^2Y_{2m}(\hat{\xi}) - 4y^2Y_{2m}(\hat{y})\right]\mathcal{U}^D_{MM'}(m)\,. \quad (46)$$

Using the symmetry relations $\mathcal{M}^D_{00}$ can be reduced to a shorter expression

$$\mathcal{M}^D_{00} = \mathrm{Re}\left(\sum_{m=0}^{2}\left[x^2Y_{2m}(\hat{x}) + \xi^2Y_{2m}(\hat{\xi}) - 4y^2Y_{2m}(\hat{y})\right]\mathcal{U}'^D_{00}(m)\right)\,. \quad (47)$$

The most important D-wave effects arise from interference with the S wave. We list the $\mathcal{U}^D_{MM'}(m)$ only for these cases:

$$\mathcal{U}^D_{1-1}(0) = \frac{1}{2\sqrt{3}}\left(\frac{U(x)U(\xi)}{\sqrt{10\pi}} + \frac{1}{5}\left[V_0(\mathbf{x},\boldsymbol{\xi}) + \sqrt{\frac{2\pi}{5}}W(x)W(\xi)\sum_{m=0}^{2}(6-5\delta_{m0})Y_{2m}(\hat{x})Y_{2-m}(\hat{\xi})\right]\right)\,, \quad (48)$$

$$\mathcal{U}^D_{1-1}(1) = \frac{\sqrt{3}}{10}W(x)\left(U(\xi)Y_{21}(\hat{x}) + \sqrt{\frac{2\pi}{5}}W(\xi)\left[Y_{21}(\hat{x})Y_{20}(\hat{\xi}) + \sqrt{6}Y_{22}(\hat{x})Y_{2-1}(\hat{\xi})\right]\right)\,, \quad (49)$$

$$\mathcal{U}^D_{1-1}(2) = \frac{\sqrt{3}}{5} W(x) Y_{22}(\hat{x}) \left[U(\xi) + \sqrt{\frac{2\pi}{5}} W(\xi) Y_{20}(\hat{\xi}) \right] , \tag{50}$$

$$\mathcal{U}^D_{1-1}(-m) = \mathcal{U}^D_{1-1}(m, x \leftrightarrow \xi, Y_{lm'}(\hat{x}) \leftrightarrow Y_{l-m'}(\hat{\xi})) . \tag{51}$$

The structure of the nine-dimensional integral in Eq. (39) becomes very complicated if short range correlations are taken into account in the ground state wave function. Therefore, as in the form factor calculations we have evaluated the integral using the Monte Carlo method.

IV. RESULTS AND DISCUSSION

To establish a perspective for viewing the effects of correlations and FSI's in our model we first discuss some aspects of a more naive model in which both these effects are absent. In particular we use an uncorrelated ground state and the plane wave impulse approximation (PWIA) for the final state. The first point we wish to establish through the use of this simple model is that, for the kinematical situation of parallel kinematics, the longitudinal response is the dominant part of the cross section. Figure 3 shows the angular distribution of the four structure functions for the highest momentum transfer ($q^2_\mu = 4.79$ fm^{-2}, $E_{\rm c.m.} = 35$ MeV) of the NIKHEFK kinematics [7] discussed in our previous publication [18]. At this setting, which corresponds to nearly parallel kinematics, i.e., $\theta_d \sim 15°$, one can see that the longitudinal response dominates the cross section at all angles. All results in this paper are given for kinematical situations where the longitudinal structure function continues to dominate the cross section. In this regard it should be pointed out that a particular feature of the ^{4}He$(e,e'd)d$ reaction is that because it is a pure isoscalar transition the lowest order exchange currents will not contribute to the transverse structure functions.

In addition to using a simple model for illustrating the relative order of magnitude of the various structure functions we also employ it to illustrate the role of antisymmetrization, i.e., the importance of the exchange terms E in Eq. (7). In Fig. 3 we also show how the longitudinal structure function depends on this quantity. One sees that whereas the direct matrix element D dominates at forward angles, as expected, the exchange term starts to become important at relatively small angles, in this instance at about 30°. For this reason, although we always include the exchange term E in our calculations, we will only show results for $\theta_d = 0$. This might be the course of action to take with heavier nuclei where E could be more difficult to assess.

We present our results as follows: For a fixed value of the kinetic energy of relative motion of the two deuterons we show, separately, results for energy transfers to the left of the quasielastic (QE) peak for deuteron emission ($\omega < \frac{q^2}{2M_D}$) and again for the right hand side of the QE peak ($\omega > \frac{q^2}{2M_D}$). The first case allows for investigation of the structure functions for very high values of the missing momentum, $p_m = |\mathbf{p}_m| = |\mathbf{p} - \mathbf{q}|$, while the range of p_m is restricted by the photon point in the latter case. As in the case of one-body knock-out reactions it is the study of the dependence of matrix elements on p_m which is expected to reflect most clearly the effect of dynamical correlations. In the following we investigate deuteron center of mass energies ($E_{\rm c.m.} = \hbar^2\kappa^2/M_d$) varying from 10 to 200 MeV. Also, when quantities are shown as a function of p_m we have plotted the curves using a step size for p_m of 0.25 fm^{-1}. Sample errors due to the Montecarlo integration are illustrated for all kinematics, although not for all curves, since the size of the error is very similar within one kinematical setting.

Figure 4 depicts the longitudinal structure function for $E_{\rm c.m.} = 10$ MeV as a function of p_m for kinematics to the left of the QE peak. Central correlations are seen to show considerable effects only for $p_m > 2$ fm^{-1} where they increase the form factor by one order of magnitude or more. The further inclusion of noncentral correlations leads to a marked change in shape of the curves with the apparent development of a minimum near $p_m = 1.5$ fm^{-1}. This minimum appears to shift to lower p_m as the D-wave percentage increases. The change in shape seems to be due only to noncentral effects. Thus although the inclusion of FSI's slightly changes the slope, they do not introduce any minimum structure into the curves. This is a promising landscape for further experimental work since we have presented a situation where short range effects are considerable at high p_m, where FSI effects do

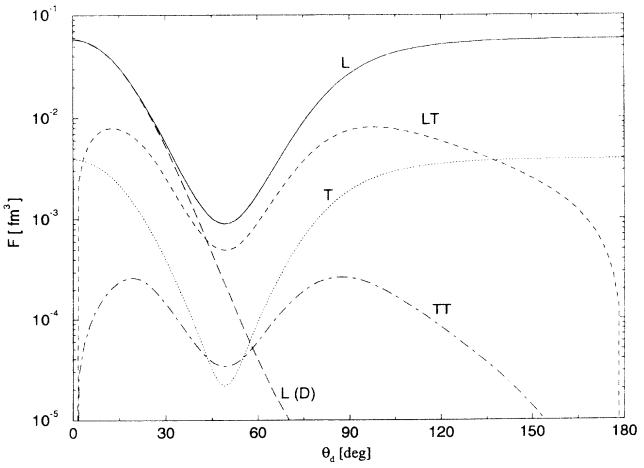

FIG. 3. Angular distribution of the four structure functions F_L (solid curve), F_T (dotted curve), F_{LT} (dashed curve), and F_{TT} (dash-dotted curve) at $E_{\rm c.m.} = 35$ MeV and $q^2_\mu = 4.79$ fm^{-2} (PWIA, no correlations). $F_L(D)$ is the longitudinal structure function when exchange contribution is neglected.

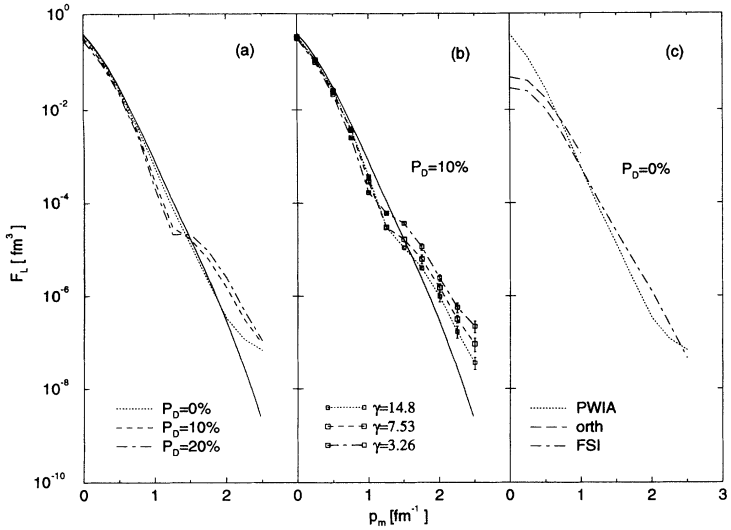

FIG. 4. Various effects on F_L at $E_{\text{c.m.}} = 10$ MeV and $\theta_d = 0°$ as a function of the missing momentum p_m at the left of the QE peak. (a) Various D-wave admixtures, i.e., model 1 (dotted curve), model 3 (dashed curve), and model 5 (dash-dotted curve). (b) Constant P_D of 10% and variable strength of short range correlations, i.e., model 4 (dotted curve), model 3 (dashed curve), and model 2 (dash-dotted curve). (c) PWIA (dotted curve), orthogonalized PWIA (dashed curve), and FSI (dash-dotted curve) for model 1. The solid curve in (a) and (b) depicts the uncorrelated PWIA.

not appear to be too strong, and moreover where the presence of tensor correlations seems to give a definite character to the curves. Confirmation of these conclusions by a proper quantum mechanical treatment of the four-body bound state and continuum is desirable but improbable in the near future.

Figure 5 illustrates the longitudinal structure factor for $E_{\text{c.m.}}$=50 MeV and energy transfers to the right of the QE peak. One sees that F_L appear as bell shape curves whose height is determined by the strength of central and tensor correlations while the latter seems to determine the position of the maxima. Figure 4(c), at low p_m, and in particular Fig. 5(c) show a very strong reduction due to FSI's. A large part of this effect can be explained by the lack of orthogonality in the PWIA. This becomes evident in both figures if a simple orthogonalization procedure is employed, i.e., $j_0(\kappa y) \rightarrow \sin[\kappa y + \delta(\kappa)]$ with suitable $\delta(\kappa)$ (see curves labeled "orth"). We have previously pointed out the importance of orthogonalization in [18], where we studied the role of FSI's for the kinematics of the NIKHEFK experiment [7]. Since the effect is only important at moderate values of $E_{\text{c.m.}}$ and q, it will not be discussed for the following cases where we consider higher $E_{\text{c.m.}}$.

The kinematics on the right of the QE peak presents comparatively more interesting results as $E_{\text{c.m.}}$ increases. For $E_{\text{c.m.}}$=150 MeV Fig. 6 shows how short range effects induce a displacement of strength in the structure functions towards lower missing momenta. This results in a quenching which can be considerable close to the photon point. FSI's amplify these effects, but the form of the curves remains unchanged. On the contrary noncentral effects create a minimum between p_m equal to 1 and 1.5 fm^{-1}, whose position as well as the height of the second maximum are ruled by the D-wave percentage. Such a minimum occurs because of a cancellation between S-wave and S-D-wave interference contributions. Changing the sign of the D wave gives rise to a maximum instead [see Fig. 7(a)]. Studying the structure function in this kinematical region would allow an independent experimental check of the sign of the D wave.

By fixing the D-wave admixture and increasing the strength of the short range correlation one simply increases the depth of the minima but does not displace

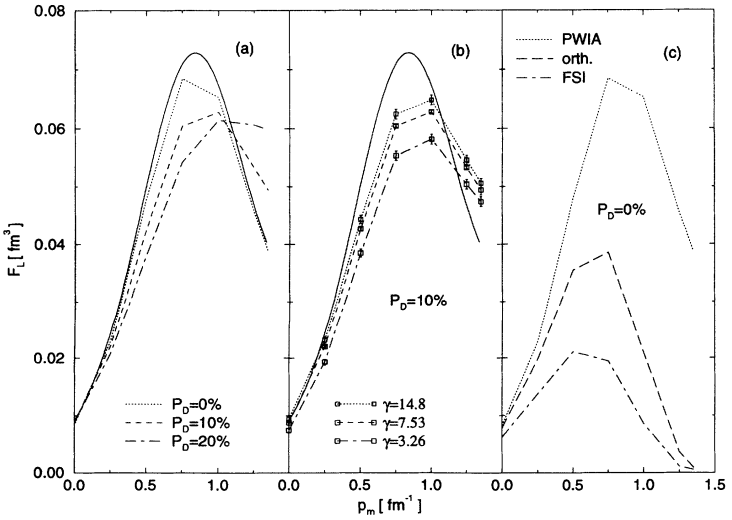

FIG. 5. As Fig. 4 but at $E_{\text{c.m.}} = 50$ MeV and at the right-hand side of the QE peak.

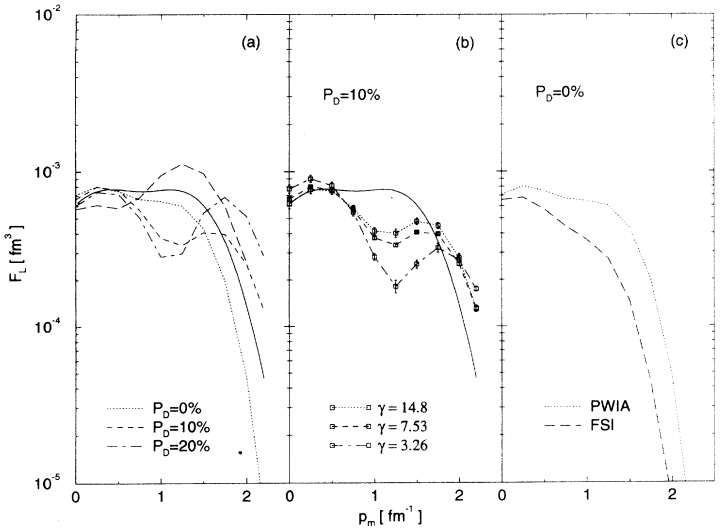

FIG. 6. As Fig. 4 but at $E_{\text{c.m.}} = 150$ MeV and at the right-hand side of the QE peak [result for orthogonalized PWIA not shown in (c)]. The long-dashed curve in (a) is obtained with a negative ϵ [see Eq. (26)].

its position. This effect shows up more clearly if we look at the $E_{\text{c.m.}}$=200 MeV case as given in Fig. 7. There one sees for the case with no D wave that short range correlations create a minimum at $p_m \approx 2$ fm^{-1}. However this minimum is markedly shifted to lower p_m by the presence of noncentral correlations. This behavior is reminiscent of a similar D-state-induced shift to the left which occurs in the elastic form factor computed earlier. A similar shift occurs in the elastic magnetic form factors of the trinucleons. The reason why it did not appear in the case of $E_{\text{c.m.}}$=150 MeV is simply a limitation of the photon point, which restricts the physical range of investigation to lower values of p_m. Again as in the case of $E_{\text{c.m.}} = 150$ MeV, once the D-wave percentage is fixed the strength of the short range correlation determines the depth of the minima, but not their position.

Following the above discussion of our results for the ^{4}He$(e,e'd)d$ reaction we comment on a technical point, namely, the convergence of the cluster expansion of Jastrow correlations. This convergence will be an important consideration when similar calculations are attempted in heavier nuclei, where a full Jastrow calculation will become increasingly prohibitive with increasing mass number A. The ^{4}He nucleus is probably a good test case because of its high nuclear density. For this test we define the first order correlated wave function as

$$\Psi_1 = N_1 \left[1 + \sum_{i<j} g(r_{ij}) \right] \Phi_0 , \tag{52}$$

the second order correlated wave function as

$$\Psi_2 = N_2 \left[1 + \sum_{i<j} g(r_{ij}) + \sum_{i<j} \sum_{\substack{m<n \\ m>i \\ (ij)\neq(mn)}} g(r_{ij}) g(r_{mn}) \right] \Phi_0 , \tag{53}$$

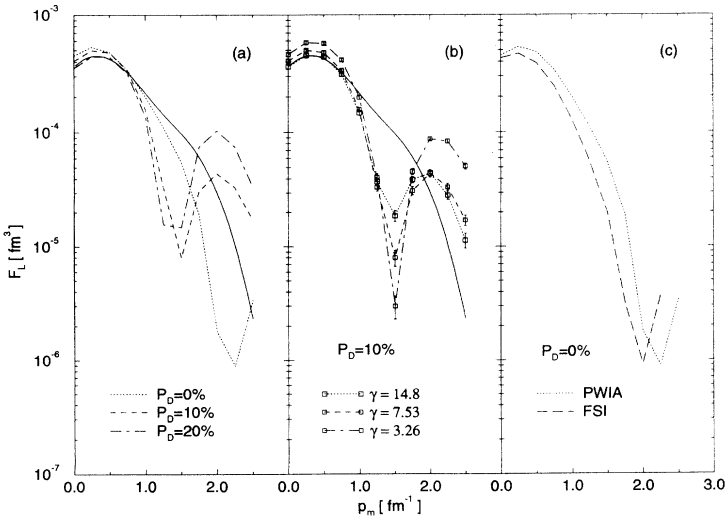

FIG. 7. As Fig. 4 but at $E_{\text{c.m.}} = 200$ MeV and at the right-hand side of the QE peak [result for orthogonalized PWIA not shown in (c)].

etc., where $g(r) = e^{-\gamma\alpha^2 r^2}$. In each case we treat the wave functions as if they were exact; that is, the normalization constants and other quantities are calculated at the same orders of $g(r)$. The approximation Ψ_1 gives more than 97% of the complete Jastrow result up to $p_m = 1$ fm^{-1}. That percentage decreases to 88% at $p_m = 2$ fm^{-1}. About half of the remaining difference to the full calculation is then recovered by the second order. Thus we conclude that for the case of heavier nuclei a second, or even a first order, Jastrow calculation would be sufficient to describe the effects of correlations.

In summary our results show that there are various interesting effects due to short range and tensor correlations in the ^{4}He$(e,e'd)d$ reaction. Particularly interesting is the increase of the longitudinal structure function at high p_m due to central correlations for the kinematics, on the left of the QE peak. Similar to the one-body knock-out case this sensitivity to short range correlations is probably reminiscent of the analogous sensitivity of the two-nucleon center of mass momentum distribution to the same effects. However, the link between the cross section and the two-body momentum distribution cannot be established.

We have found an interesting feature of the longitudinal structure function caused by the D-wave admixture, i.e., the minima which appear on the left as well as, and even more pronounced, on the right of the QE peak. The search for and study of these minima in ^{4}He as well as in heavier systems could provide information on dynamical correlations of tensor character. They would also allow an independent experimental check on the sign of the D wave in ^{4}He. Finally, with regard to central correlations, we could show that the various orders of the Jastrow calculations converge rapidly, which is an important fact for similar calculations with heavier nuclei.

In spite of the simplified model used for the reaction, particularly the lack of coupling to other channels in the final state, these results can be a useful guide for future theory and experiments.

ACKNOWLEDGMENTS

This work was supported by NATO Collaborative Resesarch Grant No. N.901003. E.L.T. acknowledges support by the National Science and Engineering Research Council of Canada. W.L., G.O., and M.T. acknowledge the warm hospitality shown at the Saskatchewan Accelerator Laboratory, where a large part of this work was performed.

[1] *Two-nucleon Emission Reactions*, edited by O. Benhar and A. Fabrocini (Editrice Tecnico Scientifica, Pisa, 1990).
[2] F.H. Heimlich *et al.*, Nucl. Phys. **A228**, 478 (1974).
[3] J.P. Genin, J. Julien, M. Rambaut, C. Samour, A. Palmieri, and Vinciguerra, Phys. Lett. **52B**, 46 (1974).
[4] W. Kratschmer, Nucl. Phys. **A298**, 477 (1978).
[5] P.H.M. Keizer *et al.*, Phys. Lett. **157B**, 255 (1985).
[6] R. Ent *et al.* Phys. Rev. Lett. **57**, 2367 (1986); **62**, 24 (1989).
[7] R. Ent, H.P. Blok, J.F.J. van den Brand, H.J. Bulten, E. Jans, L. Lapikas, and H. Morita, Phys. Rev. Lett. **67**, 18 (1991); R. Ent, Ph.D. thesis, Vrije Universiteit, Amsterdam, 1989.
[8] M. Jodice *et al.*, Phys. Lett. B **282**, 31 (1992).
[9] D.H. Beck, Phys. Rev. Lett. **64**, 268 (1990).
[10] K. Gottfried, Nucl. Phys. **5**, 557 (1958).
[11] E. Gerjuoy and J. Schwinger, Phys. Rev. **61**, 138 (1942).
[12] R. Schiavilla, V.R. Pandharipande, and D.O. Riska, Phys. Rev. C **41**, 309 (1990).
[13] B.C. Karp, E.J. Ludwig, W.J. Thompson, and F.D. Santos, Phys. Rev. Lett. **53**, 1619 (1984).
[14] R. Schiavilla, V.R. Pandharipande, and R.B. Wiringa, Nucl. Phys. **A449**, 219 (1986).
[15] J. Piekarewicz and S.E. Koonin, Phys. Rev. C **36**, 875 (1987).
[16] H.R. Weller, Nucl. Phys. **A508**, 273c (1990).
[17] M. Lacombe, B. Loiseau, J.M. Richard, R. Vinh Mau, J. Côté, P. Pirès, and R. de Tourreil, Phys. Rev. C **21**, 861 (1980).
[18] W. Leidemann, G. Orlandini, M. Traini, and E.L. Tomusiak, Phys. Lett. B **279**, 212 (1992).
[19] R.F. Frosch *et al.*, Phys. Rev. **160**, 874 (1968).
[20] R.G. Arnold *et al.*, Phys. Rev. Lett. **40**, 1429 (1978).